Mapping the inundated area caused by the July 2018 Western Japan torrential rain using multi-temporal ALOS-2 data

Wen Liu
Graduated School of Engineering
Chiba University
Chiba, Japan
wen.liu@chiba-u.jp

Fumio Yamazaki
Graduated School of Engineering
Chiba University
Chiba, Japan
fumio.yamazaki@faculty.chiba-u.jp

Yoshihisa Maruyama
Graduated School of Engineering
Chiba University
Chiba, Japan
ymaruyam@faculty.chiba-u.jp

***Abstract*—Successive heavy rainfall affected the western Japan from the late June to the early July 2018. Increased river water overflowed and destroyed river banks, which caused flooding in vast areas. In this study, two pre-event and one co-event ALOS-2 PALSAR-2 images were used to extract inundation areas in Kurashiki and Okayama Cities, Okayama Prefecture, Japan. First, the difference between the pre-event and co-event coherence values was calculated. The decreased coherence areas were extracted as possible inundation. Then the water regions were extracted by the threshold values from the three-temporal intensity images. The increased water regions in July 2018 were obtained as inundation. Finally, the extracted results from the coherence and intensity images were merged to create an inundation map. The results were verified by comparing with a web-based questionnaire survey report and visual interpretation of aerial photos.**

Keywords—land-cover map, PALSAR-2, SAR backscatter, coherence, inundation

I. INTRODUCTION

Due to a stationary seasonal Baiu (seasonal rain) front and the typhoon Prapiroon (No. 7 in 2018), multiple rounds of heavy rainfall occurred in Kyushu, Shikoku and western Honshu regions, Japan, from June 28 to July 8, 2018. The emergency heavy rain warnings were issued in eleven prefectures by Japan Meteorological Agency (JMA), which remarked the highest level of warning since its implementation. Okayama Prefecture is one of the worst affected areas; 11 out of 25 observation points of the Automated Meteorological Data Acquisition System (AMeDAS) recorded more than 400 mm cumulative precipitation from July 3 to July 8 [1]. Due to mostly by floods, 61 people were killed and three were missing in the prefecture. More than 4,400 buildings were collapsed or severely damaged, and about 9,000 were flooded [2].

Remote sensing is useful to grasp damage situations in a wide range. Among satellite sensors, synthetic aperture radar (SAR) sensors are more powerful than optical sensors to extract flooded areas after heavy rainfalls because SAR can observe day- and night-time even under cloud-cover conditions. In this study, we attempt to extract the inundated areas in Kurashiki and Okayama Cities in Okayama Prefecture using pre- and co-event ALOS-2 PALSAR-2 images. The obtained result is compared with a web-based questionnaire survey report and other references to verify its accuracy.

II. THE STUDY AREA AND IMAGERY DATA

Figure 1(a) shows the 24-hour cumulative precipitation until July 6, 2018. A half of Japanese territory suffered from heavy rainfall of more than 100 mm. It reached 138.5 mm in Kurashiki City, the second highest value in the history at this location. As the water level raised in Oda and Takahashi rivers, the breaks of the river bank occurred at three locations, which caused extensive inundation in the Mabi town area. At first, the heavy rain warning was issued for Kurashiki City at 18:30 (local time), July 5. Then the flood warnings of Takahashi and Oda rivers were issued sequentially in between 20:00 and 22:20, July 6. Evacuation advisory was announced for the whole Mabi town at 22:00, July 6. On early July 7, several overflows and breaking of banks occurred, and 70 % of the total area of Mabi town were inundated [3].

ALOS-2 made an emergency observation in the descending path at 00:05 of July 8, 2018, 24-hours after the bank breaks. The coverage of the ALOS-2 observation is shown in **Fig. 1(b)**. In the same path, two latest archive data were taken on March 18, 2017 and on April 17, 2018. These images were acquired in the StripMap 1 mode with a 3-m spatial resolution by the HH polarization. The original images were Single Look Complex (SLC) data in the processing Level 1.1. After multi-look processing (2 looks in each direction), the amplitude images were geocoded by a 5-m digital elevation model of the Geospatial Information Authority of Japan (GSI) with spacing of 5.0 m/pixel. The backscattering intensities (sigma naught values) were obtained after the radiometric calibration.

The study area was set as the red frame in **Fig. 1(b)**, including Kurashiki and Okayama Cities. The color composite of the two pre-event and one co-event images after the pre-processing steps is shown in **Fig. 2**. Since the two pre-event images were taken in the same season, the backscatter values in these images were similar and show cyan color in the color composite. Thus, the cyan areas in **Fig. 2** represent the decrease of backscatter in the co-event image. Five areas were remarked by yellow squares in **Fig. 2**, where the area I is the central part of Mabi town, Kurashiki City, which was widely flooded due to the overflows and bank breaks. The areas II to V are in Okayama City, with no news of significant flooding. The decrease in the backscatter can be seen in many locations in the figure. The areas II, IV, and V are mainly urban land-use with high backscatter and a significant decrease of backscatter could not be observed from the color composite. The area III is agriculture lands, which shows cyan color widely.

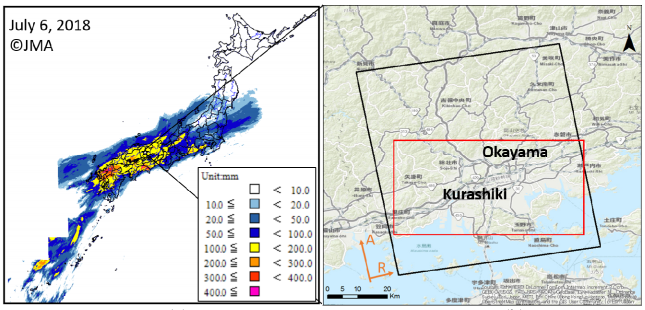

(a) (b)

Fig. 1. 24-hour cumulative precipitation until July 6, 2018 (a) and the coverage of the ALOS-2 PALSAR-2 images in Okayama Prefecture (b).

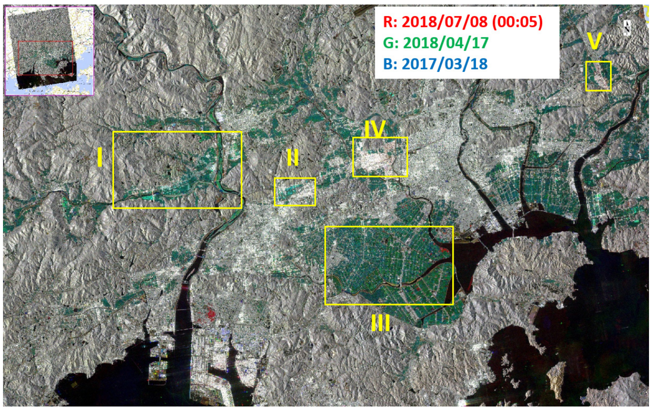

Fig. 2. Color composite of the two pre-event and one co-vent PALSAR-2 sigma naught images for Kurashiki and Okayama Cities.

III. Extraction of Inundation by Coherence Changes

The interferometric coherence is considered to be effective to extract floods in either rural or urban areas [4, 5]. Thus, the pre- and co-event coherences were calculated from the three temporal PALSAR-2 complex data. The image on April 17, 2018 was set as the master and the other two images were set as slaves. The color composite of the pre- and co-event coherences is shown in **Fig. 3**. Similar to the colors in **Fig. 2**, the cyan areas represent the decrease of coherence after the flood. A 10-m land-cover map was introduced to help the interpretation of situation in **Fig. 3**. The land-cover map was produced using multi-temporal ALOS AVNIR-2 data [6] and published digitally by JAXA [7]. The land cover was classified into 10 classes: water, urban, rice paddy, crop, grass, deciduous broad-leaved forest (DBF), deciduous needle-leaved forest (DNF), evergreen broad-leaved forest (EBF), evergreen needle-leaved forest (ENF), and bare land. The land-cover map in the target area is shown in **Fig. 4**.

The coherence in urban areas was high and stable, as shown by white color in **Fig. 3**. Since the temporal baseline of the co-event coherence (4 months) was shorter than that of the pre-event pair (1 year), the co-event coherence values in vegetated areas (grass and forest) were mostly higher than the pre-event ones and thus are seen in red color. In the area I of Mabi town, the decrease of coherence can be observed widely, similar as in **Fig. 2**. The built-up areas II, IV and V show more cyan colors than those in **Fig. 2**, which indicates the possibility of flooding.

The area III show low values in both the pre- and co-event coherences. Since no significant decrease in coherence

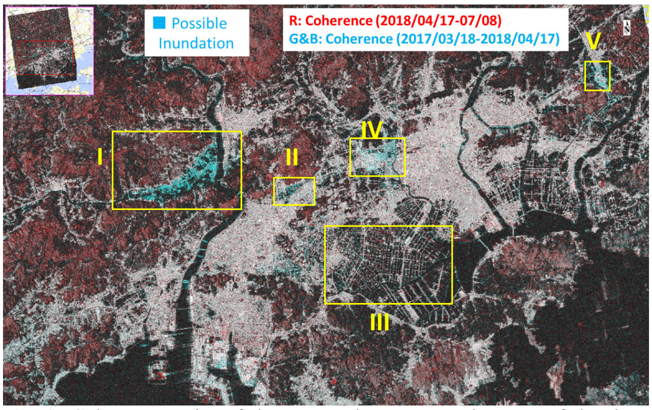

Fig. 3. Color composite of the pre- and co-event coherence of the three temporal PALSAR-2 data.

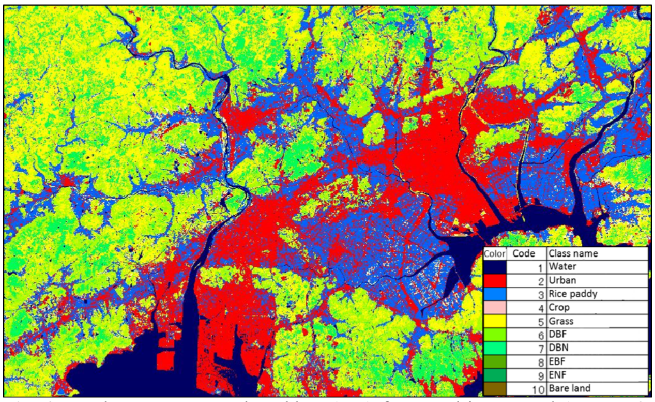

Fig. 4. Land-cover map produced by JAXA from multi-temporal AVNIR-2 optical satellite data [6,7].

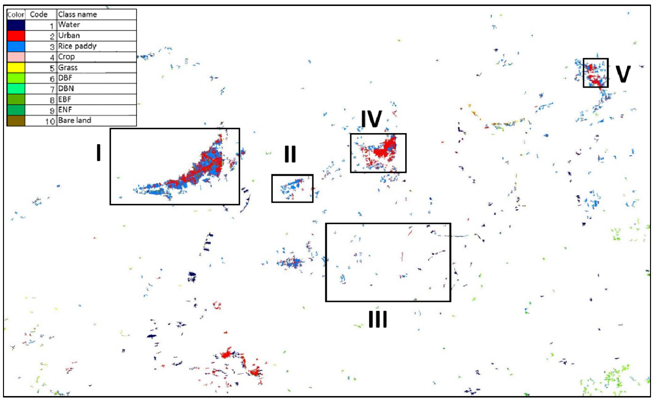

Fig. 5. Extracted inundation areas using the difference of the pre- and co-event coherence values. Colors indicate the land cover by JAXA.

can be seen in this area and the roads between agriculture fields show high coherence, the possibility of flooding in this area is low. The decreases of backscattering intensity shown in **Fig. 2** are considered to be caused by irrigating water to the rice paddy fields after the acquisition of the 17 April 2018 image. Thus, the coherence difference is considered to be more effective than the intensity difference to extract inundation, especially for rice paddy fields.

To extract inundated areas, the difference between the pre- and co-event coherences was calculated by subtracting the pre-event value from the co-event value. The average value of difference ($\mu_{\Delta\gamma}$) in the whole study area was 0.04 dB, and the standard deviation ($\sigma_{\Delta\gamma}$) was 0.16 dB. The areas with the difference lower than -0.12 ($\mu_{\Delta\gamma} - \sigma_{\Delta\gamma}$) were extracted as inundation. To reduce the noise, the extracted areas smaller than 0.01 km^2 (400 pixels) were removed from the result.

The total area of 29.8 km^2 was extracted as inundation, occupying 1.8% of the study area. The land covers of the inundation areas are shown in **Fig. 5**, mainly consisted of urban land use and some rice paddy fields. The wide inundations were detected in the areas I, II, IV and V.

IV. Extraction of Inundation by Intensity Changes

The extraction of inundation areas was also carried out using the backscattering intensity (sigma naught). The extraction using the coherence difference requires at least two pre-event images. In the case of lacking archive data, the threshold method using the backscattering intensity is still useful. Water regions were extracted from each PALSAR-2 intensity image by a respective threshold value. The threshold values were determined by sampling existing water regions [8]. The average value (μ_{water}) and the standard deviation (σ_{water}) of the sample water regions were calculated for each intensity image. The threshold value was set as $\mu_{water} + 2\sigma_{water.}$ Since the three images were taken in the same acquisition condition, the obtained threshold values were similar, -9.7 dB on March 18, 2017 and July 8, 2018, -10.4 dB on April 17, 2018, respectively.

The color composite of the extracted water regions is shown in **Fig. 6**. The existing water regions in the land-cover map was masked in the result. Besides the additional water regions shown in blue colors, a large amount of rice paddies were extracted as water from the pre-event images (white colors). We masked the pre-event water regions from the co-event ones to detect the additional water regions. After removing the areas smaller than 0.01 km^2, a total of 36.3 km^2 area was extracted as inundation. The land covers of the extracted inundation regions are shown in **Fig. 7**. Different from the result obtained by the coherence difference in **Fig. 5**, the most of the extracted areas were rice paddies. Some inundation pixels were extracted from the areas I, II, III and IV, whereas almost no inundation in the area V.

V. Verification

A map of the maximum inundation depth is shown in **Fig. 8**, which was created according to an emergency questionnaire survey by Weathernews Inc. [9] on July 7, 2018. The inundation depths were classified into 4 levels: above waist (purple), above knee (red), above ankle (yellow) and a large puddle (blue).

In the area I of Mabi town, only one person reported the inundation depth above waist. Since Mabi town was flooded from early July 7, the residents were forced to evacuate and could not answer the survey. In the area II, the inundation was extracted from both the intensity and coherence difference. There are three points showing the depth higher than knee. In the area III, no inundation was reported by the survey, which matched with the result obtained from the coherence difference. In the area IV, one point of the water depth higher than waist and eight points higher than knee were reported. In the area V, one point was reported as the water depth was higher than knee, while the considerable inundation was extracted by the coherence difference. 29% of the purple and red (above waist and knee) points were included in the inundation extracted using the coherence images, whereas 8% were included in the results using the intensity images. The difference of the SAR image acquisition time with the time of maximum water level is responsible for the omission errors. In addition, the

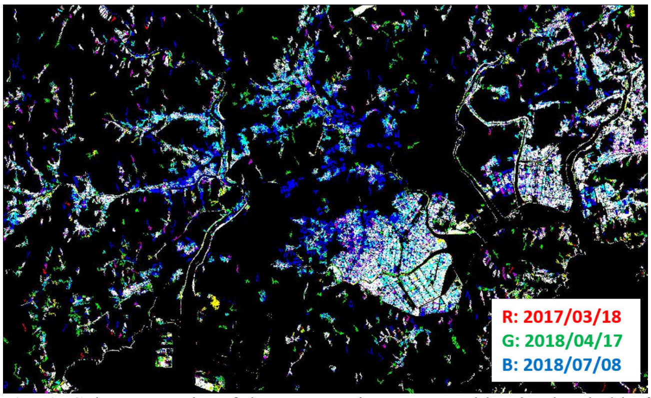

Fig. 6. Color composite of the water regions extracted by the threshold of backscattering intensity for each image.

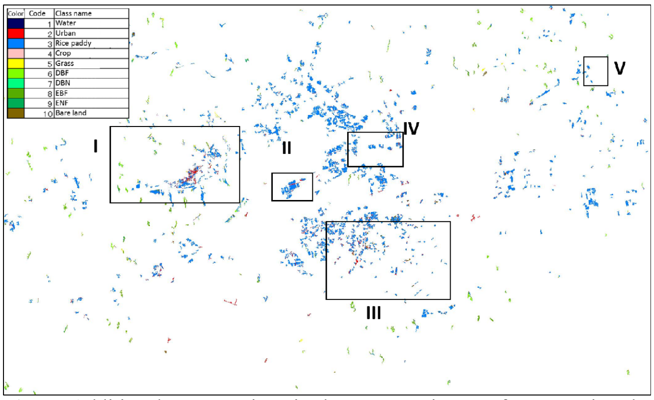

Fig. 7. Additional water regions in the co-event image after removing the pre-event water surfaces. Colors indicate land covers by JAXA.

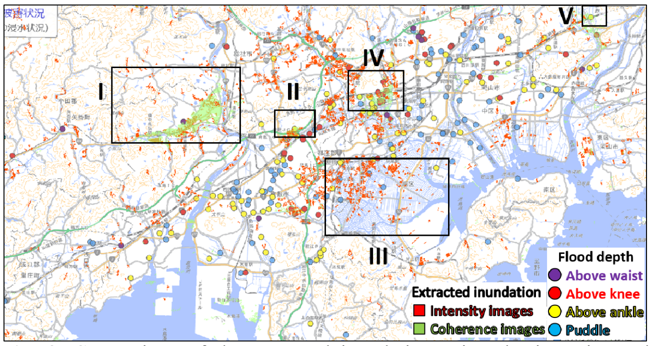

Fig. 8. Comparison of the extracted inundation using the intensity and coherence images, with an inundation map of emergency questionnaire survey by Weathernews Inc. [9] for Kurashiki and Okayama Cities.

coordinates of the questionnaire were not matched to their real locations since the responders would not answer the survey when they were flooded.

According to the comparisons in the five distinct areas, the extraction using the coherence difference showed higher accuracy than that using the threshold of the backscattering intensity for each image. However, the results from the intensity images could complement the extraction of inundation. Thus the combination of the two results was considered. An example for the area I of Mabi town is shown in **Fig. 9**. Most parts of the central Mabi town were extracted as inundation, which have a total area of 11.5 km^2.

The Geospatial Information Authority of Japan (GSI) published daily inundation maps from July 7 to 11, 2018 [3]. The inundation on July 7 was estimated according to the DEM by adding several flooding points confirmed from videos, which has a total area of 8.8 km^2. A comparison of

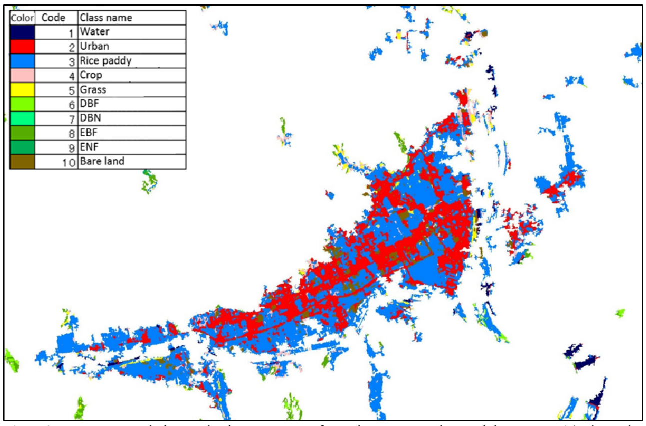

Fig. 9. Extracted inundation areas for the central Mabi town (I) by the combination of the intensity and coherence difference.

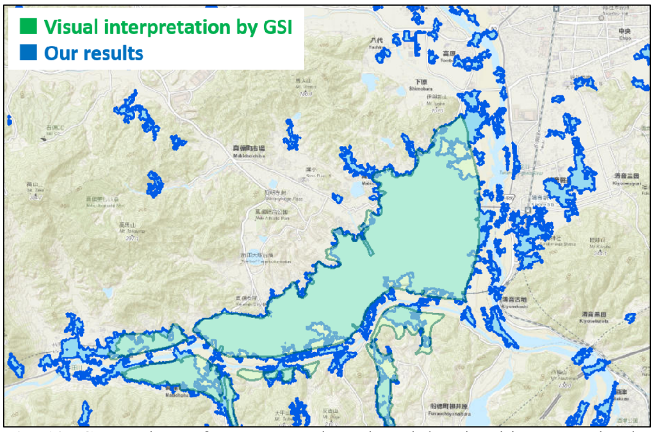

Fig. 10. Comparison of our extracted result and the visual interpretation by GSI [3].

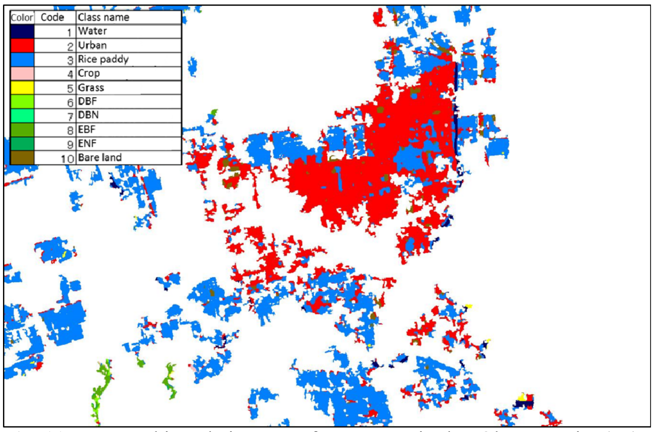

Fig. 11. Extracted inundation areas for Kume, Kita-ku, Okayama city (IV) by the combination of the intensity and coherence difference.

our result and the inundation map by GSI is shown in **Fig. 10**, which shows a good agreement. Our result included several small inundations away from the central town, which were out of the investigation map of GSI. Thus, it was difficult to confirm their accuracy.

Another example of the result in the area IV of Kume, Kita-ku, Okayama City is shown in **Fig. 11**. We visited this area on July 16, 2018 for a field survey. Although there was no significant trace of flooding left, some residents told us that the built-up areas were inundated during the heavy rainfall. Our extracted result matched with our field survey result and the questionnaire survey by Weathernews Inc.

VI. Conclusions

In this study, the inundation areas in Kurashiki and Okayama Cities, Okayama Prefecture, Japan, due to the July 2018 western Japan torrential rain, were extracted using two pre-event and one co-event ALOS-2 PALSAR-2 images. The difference between the pre- and co-event coherence values was calculated. By thresholding the difference using the combination of the average and standard deviation, the inundation areas in urban land-cover and parts of rice paddies were extracted successfully. Then the water regions in the three temporal SAR intensity images were extracted by the respective threshold value of the backscattering intensity. The additional water regions on July 8, 2018 were obtained by removing the water regions in the pre-event images. Comparing to the map of the maximum inundation depth reported by a questionnaire survey of Weathernews Inc., the extraction using the coherence was better than the one using the backscatter intensity. However, we combined those two results to obtain the final estimation. Our result showed a good agreement with the estimation made by GSI in Mabi town, Kurashiki City and our field survey in Kita-ku, Okayama City. Since the coherence difference were calculated using two pre-event and one co-event SAR images, more than three temporal images under the same acquisition are needed in our method. Thus, the proposed method could not be applied in some cases. In the future, the inundation depth will be estimated by applying our result to the high-resolution DEM.

Acknowledgment

The ALOS-2 PALSAR-2 data are owned by the Japan Aerospace Exploration Agency (JAXA) and were provided through the ALOS-2 research program (RA6, PI No.3243).

References

[1] Japan Meteorological Agency (JMA), "Weather bulletins of Okayama Prefecture on July 10, 2018," https://www.jma-net.go.jp/okayama/topix/20180710.pdf, 2018 (in Japanese).

[2] Okayama Prefectural Government, "About damage conditions until August 23, 2018 due to the July 2018 Western Japan torrential rain," http://www.pref.okayama.jp/uploaded/life/574060_4675221_misc.pdf, 2018 (in Japanese).

[3] Geospatial Information Authority of Japan (GSI), "Information for the July 2018 Western Japan torrential rain," http://www.gsi.go.jp/BOUSAI/H30.taihuu7gou.html, 2018 (in Japanese).

[4] M. Chini, L. Pulvirenti and N. Pierdicca, "Analysis and interpretation of the COSMO-SkyMed observation of the 2011 Tsunami," IEEE T. Geosci. and Remote Sensing, vol. 9, p. p. 467–571, 2012.

[5] L. Pulvirenti, M. Chini, N. Pierdicca and G. Boni, "Use of SAR data for detecting floodwater in urban and agricultural areas: the role of the interferometric coherence," IEEE T. Geosci. and Remote Sensing, vol. 54, pp. 1532–1544, 2016.

[6] S. Hashimoto, T. Tadono, M. Onosata, M. Hori and K. Shiomi, "A new method to derive precise land-use and land-cover maps using multi-temporal optical data," Journal of the Remote Sensing Society of Japan, vol. 34, pp. 102–112, 2014 (in Japanese).

[7] Japan Aerospace Exploration Agency (JAXA), "High-resolution land-use and land-cover maps," http://www.eorc.jaxa.jp/ALOS/lulc/jlulc_jpn.htm, 2017 (in Japanese).

[8] W. Liu and F. Yamazaki, "Detection of inundation areas due to the 2015 Kanto and Tohoku torrential rain in Japan based on multi-temporal ALOS-2 imagery," Natural Hazards and Earth System Sciences, vol 18, pp. 1905–1918, 2018.

[9] Weathernews Inc., "Indundation conditions in the maximum of flood depths," https://weathernews.jp/s/gensai/rain_enq201807/map.html, 2018 (in Japanese).